

Long-term stability of sensible thermal energy storage materials developed from demolition wastes interacting with hot heat transfer fluid

Burcu Koçak^{1,2}, Ana Ines Fernandez¹, Halime Paksoy^{2*}

¹DIOPMA Centre, Department of Materials Science & Physical Chemistry, Universitat de Barcelona, Martí i Franquès, 1, 08028, Barcelona, Spain

²Chemistry Department, Faculty of Arts and Sciences, Çukurova University, Balcali Mah. Saricam, 01310 Adana Turkey

*Halime Paksoy, Balcali Mah. Saricam, 01310 Adana Turkey. E-mail: hopaksoy@cu.edu.tr

Abstract

Packed-bed thermal energy storage (TES) system filled with low cost and sustainable sensible thermal energy storage material (STESM) is a promising option for medium-high temperature applications. STESM developed from demolition wastes are eco-innovative and compatible with circular economy. They can be used in solar heat industrial applications up to 750°C. One of the main concerns that should be taken into consideration is the stability of STESM developed from demolition wastes in direct contact with hot heat transfer fluids (HTF). In this study, thermal and mechanical stability of STESM developed from demolition waste were investigated using repeated heating and cooling cycles in Therminol 66 synthetic oil as HTF at 150°C for up to 500 h. The characterization results before and after thermal cycling showed that new STESM developed from demolition wastes is thermally and mechanically stable. Also, strong oil penetration into the STESM samples improved the porosity, strength and specific heat capacity. The specific heat capacity and mechanical strength values increased from 1330 J/kgC to 1490 J/kgC and from 4 MPa to 6 MPa, respectively. These results suggest that STESM samples developed from demolition waste can be used reliably in solar heat industrial applications for long term.

KEYWORDS: demolition waste, sensible thermal energy storage material, stability, thermal cycling

1.INTRODUCTION

For sustainable, uninterrupted and cost effective renewable energy supply in industrial plants sensible thermal energy storage (STES) systems is proven to be a good alternative. Number of industrial solar heat applications can be increased by integrating STES systems for a more sustainable future. Sustainability aspects of STESM make them even more favorable.

Going green in industries requires being more carbon neutral. STES systems using packed-bed technology offer industries to replace fossil fuels with solar heat at low cost while reducing their CO₂ emissions. Cost-effective and sustainable STESMs are the key elements of such systems for increased competitiveness while being green in industry.

Recent studies focus on using packed-bed TES tank filled with solid packing to provide several benefits such as reducing the usage of mineral oil and molten salts as liquid, overall cost reduction potential, simple design, environmentally friendliness [1, 2]. Solid STESMs such as silica sand, natural rock, glass, steel, alumina, quartzite and concrete were suggested as alternative low cost STESMs instead of molten salt and mineral oil for high temperature applications [3-5]. There are several studies in literature showing that such solid STESMs have good storage performance for high temperature TES applications. Although their specific heat capacities ranging from 500 Jkg⁻¹C⁻¹ to 1300 Jkg⁻¹C⁻¹ are not very high, they have excellent thermal conductivities; 1.0 Wm⁻¹K⁻¹ to 3.0 Wm⁻¹K⁻¹ for rock, concrete, basalt and 30 Wm⁻¹K⁻¹ to 40 Wm⁻¹K⁻¹ for ferrous alloys [5-12]. In addition, densities of solid STESMs are higher than liquid STES media; varying from 1700 kgm⁻³ to 7800 kgm⁻³, which give them superior volumetric heat capacities [13].

Natural solid STESMs are preferable options for STES applications due to their high thermal and chemical stability, low cost and high storage capacity [1, 4, 14]. But, in most large-scale applications, tons of STESM requirement causes depletion of natural sources.

Waste-based materials such as industrial by-products [15, 16], municipal solid wastes [17]; inertized wastes [17]; asbestos containing wastes [18, 19] and industrial furnace slags [20-24] are promising low cost and ecofriendly STESMs for high temperature industrial applications. These studies prove that STESMs developed from waste-based materials offer good thermal properties and cheapest solutions for high temperature applications. Another advantage of using such waste materials in STES is their compatibility with circular economy that is imposed by EU Green Deal in becoming climate neutral [25].

In our previous studies [26-28], demolition wastes (DW) taken from an urban regeneration project were assessed as alternative STESM in packed-bed TES system for high temperature industrial applications.

DW, which is one of the heaviest and the most voluminous waste material, is a significant problem for governments. In Europe, more than 800 million tons of DW originates from partial or total demolition of residential, commercial and municipal buildings, roads or civil infrastructures [29]. Turkey is also suffering from this solid waste. After the Law No. 6306 on Transformation of Areas under Disaster Risk, urban regeneration is increased rapidly in the last 9 years. Thus, it is estimated that construction and demolition waste amount increased from 4-5 million tons/year to 10 million tons/year in Turkey [30].

According to Turkish Waste Framework Directive (2008/98/EC) [31], at least 70 % of the non-hazardous demolition wastes should be recycled. Therefore, valorization of DW will become an important key performance indicator for municipalities.

Utilizing the most voluminous DW, which would otherwise be a big burden to the environment for energy saving purposes provides multiple benefits. In addition to reaching recycling targets for DW, especially industry sector can profit from using cost-effective, high energy density and sustainable alternative storage material for renewable energy applications.

High energy density, good heat transfer and low cost are the most relevant properties when selecting the most proper STESM candidate. Furthermore, lifetime, mechanical and chemical stability of STESM, and compatibility of STESM with heat transfer fluids (HTF) at high temperatures are important criteria to be taken into account for secure and uninterrupted operations in industry [32].

There are several studies on stability of solid STESMs for long-term applications. Martin et al. [2] investigated the long-term stability of quartzite and basalt up to 560°C to reduce cost of molten-salt based thermochemical storage system by replacing a significant amount of solar salt. Quartzite and basalt were thermally stable after thermal treatment in solar salt at 560°C for 1000 h. Jemmal et al [33] applied 110 thermal cycles to siliceous rocks in an electrical oven. Hot air was used as heat transfer fluid from 300°C to 550°C. Although no significant mass loss was observed, cracking occurred due to thermal expansion. Grirate et al. [34] studied the compatibility of quartzite pebbles and silica sand with Therminol 66 synthetic oil. No significant change was found in both oil and rocks that affects the TES system performance. Diago et al. [9] pointed out significant mass loss in desert samples due to

calcination of high content of calcite after the first thermal cycle in a furnace at 1100°C. Allen et al. [35] investigated different rock types to be used in an air based packed-bed TES system for solar power plants. A number of rock samples such as gneiss, granite, pegmatite, dolerite, sandstone, hornfelsic and greywacke were cycled approximately 950 times under air flow at temperature range of 350 - 500°C. At the end of thermal cycling, the greywacke and sandstone samples (both sedimentary rocks) withstood the thermal cycling process well and no mass loss was detected due to thermal cycling. Becattini et al. [36] assessed six types of rocks such as mafic rock, felsic rock, calcareous sandstone, limestone, quartz rich conglomerate and serpentinite from Alpine to investigate their suitability for high-temperature packed-bed TES systems. Mafic rocks, felsic rocks, serpentinite, and quartz-rich conglomerates were found as thermally and mechanically stable under air flow between 100°C and 600°C. Li et al [37] investigated the effects of thermal cycles on mechanical stability of granite and revealed that thermal cracks occur in the first cycle and slightly increase with thermal cycles. Molina et al. [3] performed ageing and compatibility test to various natural solid materials in Jarytherm® DBT oil at 340°C for 500 h. Glass, steel and alumina were determined as potential solid materials that can be used in direct contact with oil.

Py et al. [18] found that recycled industrial ceramics made by vitrification of asbestos containing wastes (ACW) is thermally stable after 2 thermal cycles at 1200°C and can be used as STESM for all kinds of CSP plants. In the study of Faik et al. [17], 2 heating/cooling cycles between room temperature to 1100°C were applied to asbestos-containing wastes and fly ashes under air-flow. Both materials were defined as suitable for high temperature CSP applications with their thermally stable structure and high total emissivity. Grosu et al [23] applied 6 heating cooling cycles to basic oxygen furnace slag, magnetite ore and river rock samples to be used as STESM in 1 MW_{el} pilot CSP plant in Morocco. Although samples were found as thermally stable under air at operation temperature range (170-320°C), Grosu et al [38] reassessed thermal and mechanical stability of the materials in direct contact with Delco Term Solar E15 oil (current HTF used in CSP plant). As a result, using basic oxygen furnace slag in direct contact with oil was not recommended due to the strong oil penetration into the material's macropores. Agalit et al [20] showed that induction furnace slags are thermally stable after three heating/cooling cycles up to 1000°C under air. Calvet et al [19] presented that Cofalit produced from asbestos containing wastes by high temperature plasma treatment at 1500°C was thermally and mechanically stable in direct contact with nitrate salt up to 500 °C in molten salt storage systems. Motte et al [39] investigated compatibility of postindustrial ceramics with

molten salt (mixture of sodium and potassium nitrates). Although asbestos containing wastes, coal fly ashes, blast furnace slags were stable in molten salt for 500 h at 500°C, direct contact of converter steel slags and electric arc furnace slags with molten salt was not recommended due to the corrosion risk.

As a conclusion of the previously reviewed literature, most of these studies were carried out for natural STESMs. There are some recent studies that show stabilities of waste based STESMs after thermal cycling. But, most of them were done with air and for short term.

Most of waste-based STESMs cannot be used as they are and need to be produced by some necessary processes such as crushing, milling, molding, pressing etc. [15, 16, 21, 26, 39, 40]. Although its chemical content varies according to the source of waste, DW mainly consists of gypsum, wood (plywood, chip wood and sawdust), masonry (brick, concrete, rock), metals, plastic and cardboard. DW's physical and chemical properties such as size, shape, density, humidity and chemical content are not uniform. As a result of DW being stored in open space, its humidity may reach to over 20 % depending on climate condition. Density of DW varies for each particle based on its composition; for bricks it is 1600 kgm⁻³ and for concrete it is 2200 kgm⁻³. Therefore, similar processes like the other waste-based materials were applied to DW to get homogeneous and rigid structure [26].

Compared with natural solid STESMs, STESMs developed from demolition waste are ecofriendly and cost effective materials. Simulation studies showed that valorization of demolition wastes as STESM to be used in packed-bed is a sustainable approach in reducing fossil fuel consumption of medium-high temperature industrial applications and increasing efficiency of CSP [41-44]. But applying extra processes can have a significant effect on thermal and mechanical behavior of STESM and their lifetime.

In this perspective, a thorough understanding of stability of the new STESM under thermal cycling is necessary. Although the STESM developed from DW was tested in a lab-scale packed-bed TES system and showed high storage efficiency in a temperature range of 120°C to 180°C [28], change in structural, chemical, thermophysical and mechanical properties of waste based STESM with cycling should be investigated for ensuring long lifetime and reliability of the TES system.

The main objective of this paper is to evaluate the potential of demolition waste for reliable and long-term use as STESM in high temperature industrial applications. The thermophysical, chemical, mechanical and structural changes of the new STESM developed from demolition waste exposed to repeated heating and cooling cycles from room temperature to 150°C for up to 500 h were investigated to assess its stability.

2.MATERIALS AND METHOD

2.1 Materials

Demolition waste samples that had a heterogeneous structure were collected from an urban regeneration project in Adana, Turkey. Homogeneous dry powders were produced from DWs by crushing, sieving, mixing and drying processes [26]. Figure 1 shows homogeneous demolition waste powders (a), spherical STESMs (b) and cubic STESMs developed from DW (c).

The new STESM was prepared by molding the DW powder with Portland cement to prepare desired geometries. The DW - CEM I 52.5 white Portland cement mass ratio of 9:1 was defined as the best mortar formulation for higher strength and storage capacity [26]. Tap water was used in preparing the mortar mixtures which were poured into cubic and spherical molds. STESM samples were dried under the sun for 8 hours and in an oven at 150 °C for 1 hour.

In this study, the cubic samples with dimensions of $50 \times 50 \times 50 \text{ mm}^3$ and spherical samples with diameter of 10 mm were produced with the method given in Koçak and Paksoy [26], where thermal, physical and chemical properties of the new STESM were shown to be suitable for low cost applications up to 750°C with high storage capacity ($4100 \text{ kJm}^{-3}\text{C}^{-1}$).

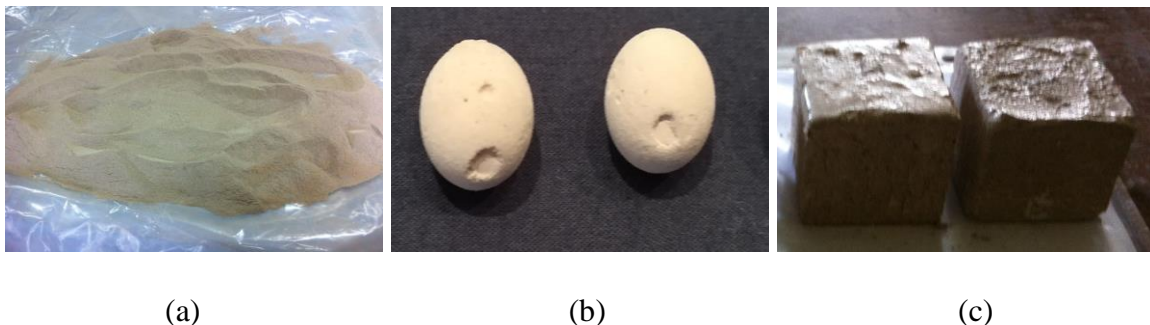


FIGURE 1. Demolition waste as STESM a) DW powder b)Spherical STESM c)Cubic STESM

In packed-bed TES systems, the considered STESM samples have to be stable with high temperature heat transfer fluid (HTF). The properties of Therminol 66 synthetic oil selected as HTF are listed in Table 1.

TABLE 1 The properties of Therminol 66 synthetic oil

Properties	Values	Unit
Density, at 25°C	1005	kgm ⁻³
Specific Heat, at 25°C	1579	Jkg ⁻¹ C ⁻¹
Maximum bulk temperature	345	°C

2.2 Thermal Cycling Tests

Eleven sets of cubic and spherical samples were prepared for thermal cycling tests. One set of the samples was not subjected to thermal cycling to characterize the sample before thermal cycling. The other 10 sets of samples were immersed in separate closed glass containers filled with Therminol 66 synthetic oil. Containers were placed into an oven (Heraeus T6420) to apply heating/cooling cycles. Temperature deviation of the oven was ± 3 °C at 150°C.

The maximum heating cycle temperature of 150°C was chosen to simulate the most common solar heat industrial process temperature range [13].

Each set of samples were immersed in separated closed glass containers filled with Therminol 66 oil and were placed into the oven. Figure 2 shows the temperature program of the oven. The oven was heated from room temperature to 150°C at a heating rate of 2°C/min, stayed at 150°C for 2 h and then it was cooled down to room temperature with a cooling rate at 2°C/min. There was no waiting time at room temperature. When the oven reached room temperature, the heating step started again.

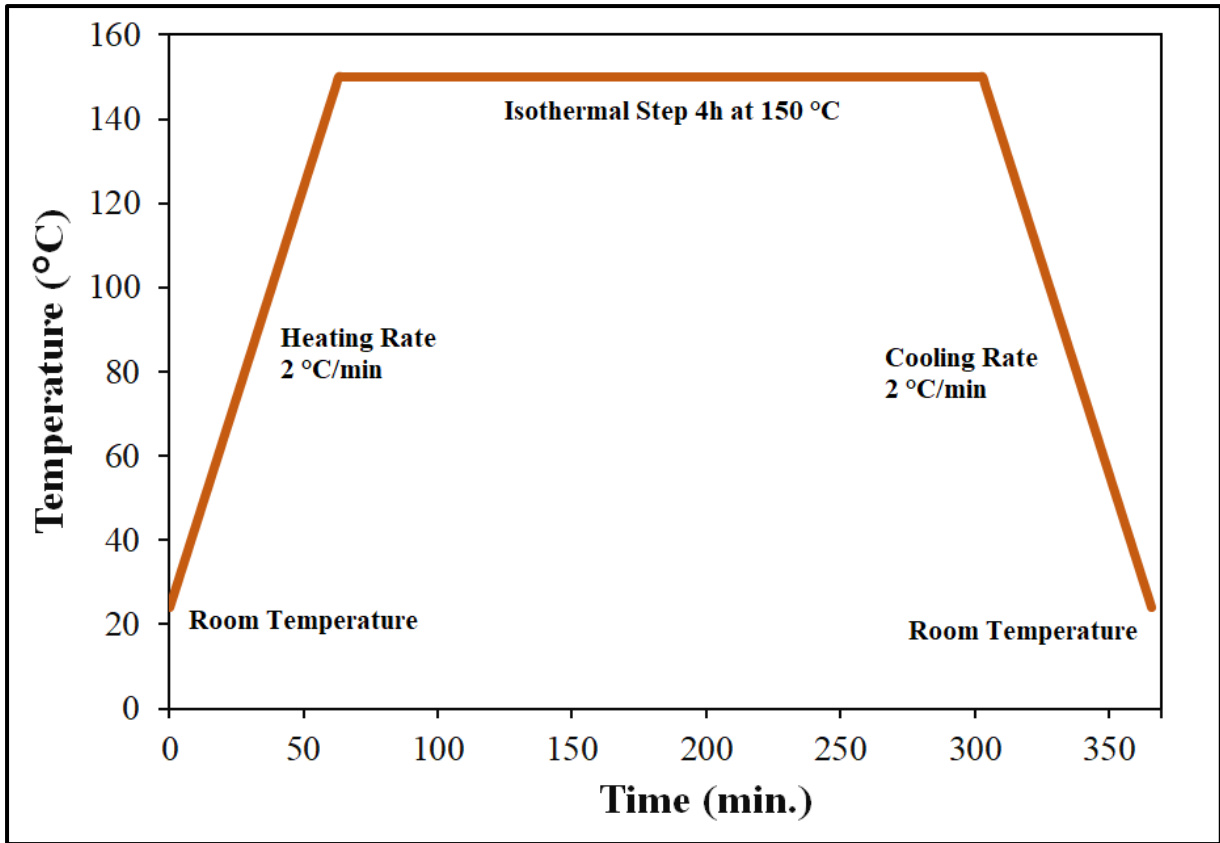


FIGURE 2. Temperature program for heating/cooling cycles

TABLE 2 Test duration of cubic and spherical set of samples

Sample No:	1.	2.	3.	4.	5.	6.	7.	8.	9.	10.	11.
Test duration, h	0	50	100	150	200	250	300	350	400	450	500

Test periods for each set of cubic and spherical samples are given in Table 2. Repeated heating/cooling cycles were performed up to 500 h. The oven had a time counter instead of cycle counter. For this reason, each set of samples was taken out from the oven at equal time intervals of 50 hours. Finally, the 10th set of samples were removed from the oven at the end of 500 h. Figure 3 shows all the samples before and after thermal cycles.

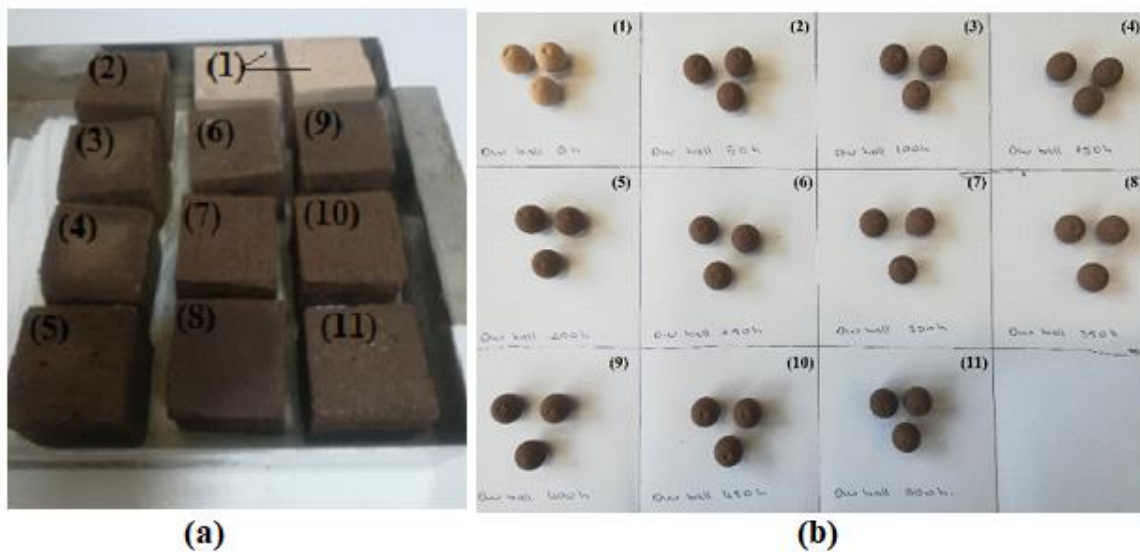


FIGURE 3 Pictures of cubic (a) and spherical (b) storage material samples before and after the tests

2.3 Characterization

Changes in structural, chemical, thermophysical and mechanical properties of samples before and after thermal cycling were analyzed in order to determine any changes.

Inner surface of spherical STESMs were imaged by Zeiss Axiovert S100 microscope at 10 X magnification. BET Surface area and porosity analysis of STESM samples were measured based on "Brunauer–Emmett–Teller" (BET) theory by TriStar 3000 V6.04 instrument. The test was carried out under pure Nitrogen flow at -196°C . Infrared spectrum of the materials were obtained by attenuated total reflectance infrared spectroscopy (FT-IR ATR) using Spectrum Two™ from Perkin Elmer. The test was applied by scanning of wavelengths from 4000 to 450 cm^{-1} . Average density of spherical STESMs was measured by gas displacement technique using AccuPyc 1330 Pycnometer automatic density analyzer. Specific heat (C_p) of STESM samples was measured using Sapphire DSC 3 Star System Mettler Toledo. DSC analysis of samples was carried out in temperature range of 25 - 500°C at a heating rate of $10^{\circ}\text{Cmin}^{-1}$. Sapphire was used as reference sample and analyses were performed using 40 mL aluminum crucibles under $50\text{ mLmin}^{-1}\text{ N}_2$ flow. Mass loss and thermal degradation behavior of packing materials were determined by SDT Q600 V20.9 Build 20 Thermogravimetric Analysis (TGA) device. Samples before thermal cycling were heated up to 1200°C at a heating rate of $20^{\circ}\text{Cmin}^{-1}$. Samples after thermal cycling were heated up to 300°C at a heating rate of 10°C under air

and stayed at 300°C for 60 minutes. TGA analysis was limited up to 300°C to prevent degradation of Therminol 66 synthetic oil that may have infiltrated in the STESM samples' structure. Mechanical strength of the STESMs was investigated by compressive strength test method. The test was applied to cubic packing materials by single axial load measurement device according to TS EN 12390-3 international standard.

3.RESULTS AND DISCUSSION

3.1 Change in Structural and Chemical Properties

The visual inspection is essential to evaluate macroscopic changes such as cracking, texture and color. Figure 4 shows the spherical samples before thermal cycling (a), after 250 h (b) and 500 h thermal cycling (c). Surface deformations or cracking were not found at the end of thermal cycling. It is apparent from Figure 4 that spherical STESMs immersed in Therminol 66 synthetic oil darkens with cycling time. Color change that takes place in the STESMs varies depending on several factors such as structure of STESM, type of HTF and temperature range. For example, in the study of Diago et al. [9] color of desert samples shifted to whiter tones due to the calcination after thermal cycling under air at 1100°C. In the case for DW, the color change can be attributed to oil penetration into the samples.

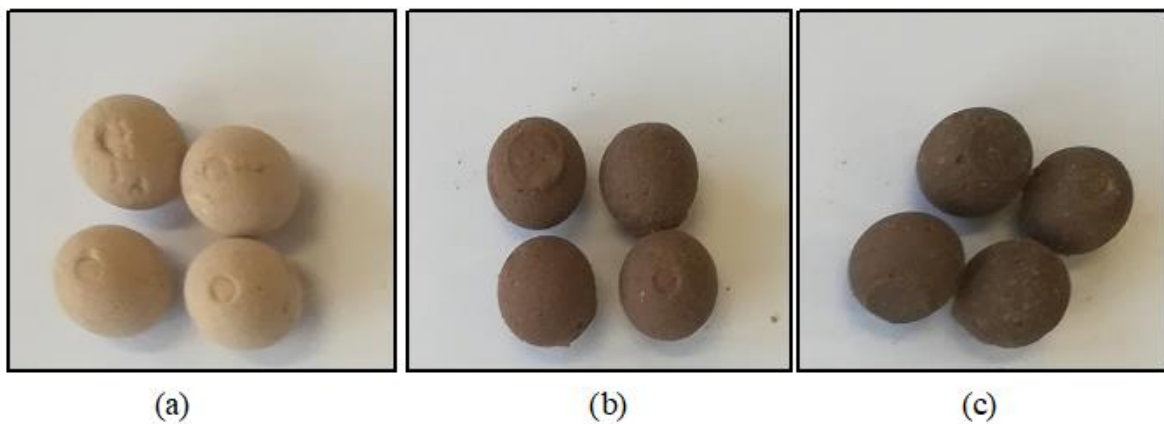


FIGURE 4 Images of spherical STESM samples; before cycling (a), after 250 h (b), after 500h (c)

Figure 5 shows the images of inner surfaces of cubic STESMs that were crushed. Oil penetration into cubic STESM samples can be easily seen. Penetration towards the center increases with time and at the end of 500 hours the oil penetrates all over the material.

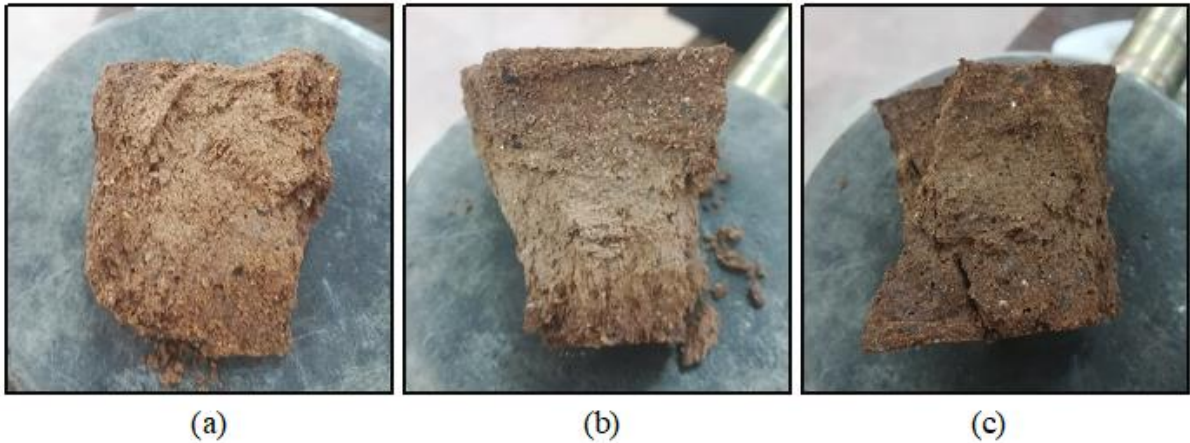


FIGURE 5 Images of inner surface of cubic test samples; 50h (a), 250 h (b), 500h (c)

Thermal cycling does not only affect the visible properties but can also change mechanical properties that affect the storage performance. In the study by Li et al. [37] micro-cracks were observed over the surface of granite sample as a result of thermal expansion at 650°C. According to Jemmal et al. [33], crack formation after thermal cycling is a significant issue that reduces mechanical strength of the STESM. They recommended using smaller sized STESM to avoid cracking. In the study of Motte et al [39], no significant crack and porosity formation were found in asbestos containing waste ceramics before and after thermal treatment in molten salt. However, some significant open porosities were found in steel slags after thermal treatment due to the corrosion of iron phases.

In this study, the spherical samples before and after thermal cycling were cut in half to observe any thermal cracks and porosities. Microscopic images of STESM (See Figure 6) were taken by Zeiss Axiovert S100 microscope at 10 X magnification. As seen in Figure 6 no new porosity and crack formations were detected after thermal cycling. However, it is clearly seen that samples get darker as the thermal cycling time increases. This is an evidence of Therminol 66 synthetic oil penetration as described in Figure 5. This shows that Therminol 66 synthetic oil penetration is not only on the outer surface of the STESM samples, but also into the inner surface. Similar oil penetration behavior was also seen in basic oxygen furnace slag. But, due to its high macro porous structure, erosions and big cracks were formed after oil penetration that prevented its use in direct contact with oil [38].

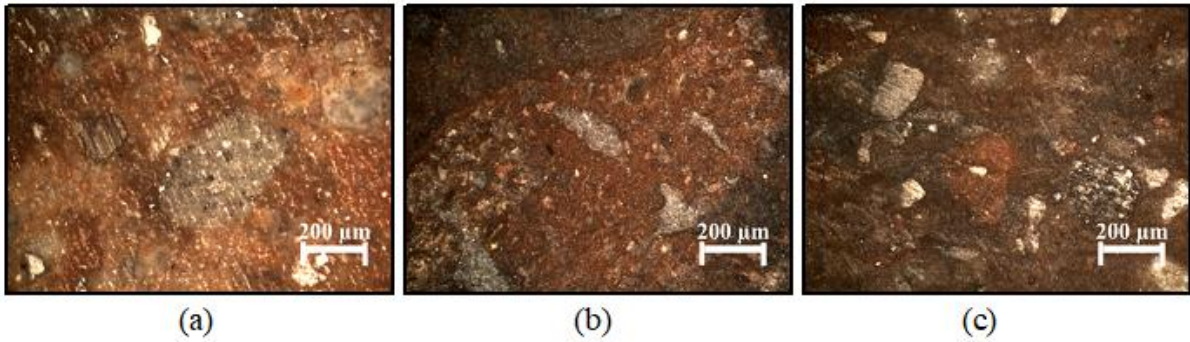


FIGURE 6 Microscopic images of packing material at 10X magnification; before cycling (a), after 250 h cycling (b), after 500 h cycling (c)

Low porosity is a preferred criterion for STESMs [33]. According to Zahir et al [45] porosity has a high influence over the mechanical and physical properties of the materials. Becattini et al [36] reported that porosity in some rock types, which contain high amount of calcite and quartz increases after thermal cycling due to the decomposition of calcite and the quartz inversion.

Surface area and porosity of spherical STESM samples (Table 3) before and after thermal cycling were measured by BET analysis. Test results showed that spherical STESM samples developed from demolition waste had very low porosity before thermal cycling. According to Chaki et al. [46] porosity of solid STESMs is expected to increase with temperature. On the contrary, BET surface area, pore width and total pore volume of the STESM samples in this study decreased after 500 h thermal cycling. This shows there was no significant enhancement of the porosity during the thermal cycling at 150°C. The average adsorption pore width decreased slightly from 242 Å to 226 Å. This may be the result of the deposition of Therminol 66 into pores of the STESM.

TABLE 3 Surface area and porosity of spherical STESM samples

Properties	Before cycling	After 500 h cycling
BET surface area	$11.6969 \pm 0.0377 \text{ m}^2\text{g}^{-1}$	$8.3733 \pm 0.0484 \text{ m}^2\text{g}^{-1}$
Molecular cross-sectional area	0.1620 nm^2	0.1620 nm^2
Average adsorption pore width	242.45 \AA	226.73 \AA
Pore volume	$0.006403 \text{ cm}^3\text{g}^{-1}$	$0.047463 \text{ cm}^3\text{g}^{-1}$

Grirate et al. [47] stated that liquid HTFs such as oil or molten salt can alter properties of STESM by penetrating into their structure. The thermal cycling study on asbestos containing wastes by Faik et al [17] reported that crystallization behavior limited the usage of inertized asbestos containing waste glass as STESM to 500°C applications.

Therefore, penetration of Therminol 66 synthetic oil into the internal structure can affect chemical properties of the STESM and it should be evaluated. FTIR analysis was carried out to determine chemical change in of STESM after thermal cycling. Figure 7 compares infrared spectra of packing materials before cycling and after 500 h cycling. At the end of thermal cycling, similar spectra were observed before and after thermal cycling with some new peaks between 2850-3050 cm^{-1} , corresponding to an organic substance as seen in the spectrum in red of Figure 7. FTIR spectra of Therminol 66 synthetic oil before cycling and after thermal cycling was examined before by Grirate et al. [34] and peaks around 2950, 2850, 1600, 1500 and 600 cm^{-1} were observed. These new peaks and the others seen after thermal cycling are compatible with the results of Grirate et al. [34], which shows the presence of Therminol 66 oil without any degradation of chemical structure.

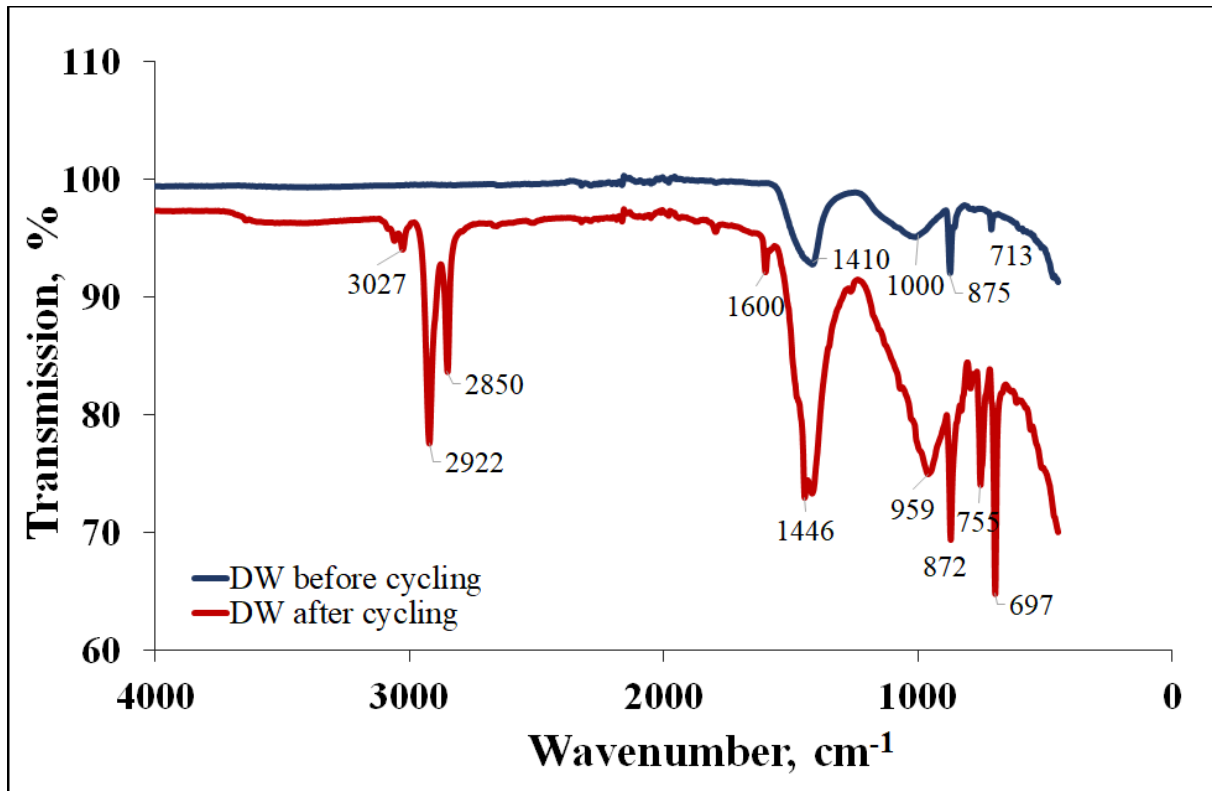


FIGURE 7 FTIR spectra STESM samples, before and after 500 h thermal cycling

3.2 Change in Thermophysical and Mechanical Properties

Densities of packing materials before and after thermal cycling are given in Table 4. Average density that was determined as 2855 kgm^{-3} before thermal cycling decreased to 2030 kgm^{-3} after 500 h of thermal cycling. This reduction in density can be explained by the deposition of Therminol 66 heat transfer oil into the pores. In the study of Baba et al [32],

density of magnetite was increased by 2.4% after thermal cycling due to the oxidation and decomposition of some organic materials at high temperature.

TABLE 4 Density of the spherical STESM samples before and after thermal cycling

Sample	Density, ρ @25 °C, kgm^{-3}
STESM before cycling	2855
STESM after 500 h cycling	2030

Specific heat capacity of STESMs may change after thermal cycling due to possible changes in chemical composition such as decomposition, dehydration, evaporation depending on the material and operating conditions. For example, in the study by Jemmal et al [33], specific heat capacity of siliceous rocks decreased more than 15% after 110 thermal cycles under air up to 550°C due to the dehydration of rocks. In another case [36], specific heat of felsic rock sample started to decrease after 100°C due to evaporation of water, which has approximately 4 times higher specific heat than rocks. Reduction in specific heat reached to 45% at cycling temperature of 550°C due to the dehydration of chlorite.

Average specific heat measurements of spherical STESM samples in this study between 80-180°C are given in Table 5. An increasing trend was observed in specific heat with increasing cycling time due to the deposition of Therminol 66 synthetic oil that have higher specific heat than demolition waste. Increasing specific heat capacity of STESM with thermal oil is beneficial in such systems due to increase in TES capacity. Xu et al [48] used sand saturated with heat transfer oil to increase the storage efficiency of TES system by 5%.

TABLE 5 Specific heat of STESM samples

Samples	Average Specific heat, C_p, $\text{Jkg}^{-1}\text{C}^{-1}$
STESM before cycling	1330
STESM after 250 h cycling	1380
STESM after 500 h cycling	1490

In this study, even if the specific heat was increased, the density decreased after thermal cycling. Although volumetric storage capacity ($\rho \cdot C_p$) of the sample seems to decrease after thermal cycling due to the lower density caused by 28% mass gain observed in the spherical samples after 500 h thermal cycling, this increase in mass due to penetrated oil will ensure that there will be no significant change in total storage capacity of the system ($m \cdot C_p \cdot \Delta T$).

As discussed above, mass of the samples changed after thermal cycling due to the oil penetration. A number of studies mention that mass loss was observed after thermal cycling up to 1000°C under air due to the calcination, decomposition of organics, dehydration etc. [2, 9, 33]. In other studies, no mass loss after thermal cycling was observed [20, 35]. In the study by Grosu et al [23], river rock and basic oxygen furnace slag samples showed minor mass loss at 170°C due to the organics decomposition and water removal. On the other hand, magnetite samples gained mass after thermal cycles because of oxidation of Fe_3O_4 to Fe_2O_3 .

In previous study by Koçak and Paksoy [26], TGA analysis showed that STESM samples developed from demolition waste lost 3-4% of mass between 100-200°C due to the humidity before any thermal cycling tests. Decomposition started at around 750°C and about 80% of inorganic content remained after 1000°C. In this study, TGA measurements were carried out on STESMs after thermal cycling. As seen in Figure 8, spherical STESM samples after thermal cycling were heated up to 300°C and then kept at 300°C for 1 hour. Unlike TGA behavior of the sample before thermal cycling, mass losses up to 15 % were observed between 200-300°C due to volatiles from Therminol 66 synthetic oil. Also, samples were kept at 300°C for 1 hour and no significant mass loss was observed. According to Jemmal et al [33] all mass losses up to 300°C occurring in the first heating cycle, is the result of evaporating of humidity. Decomposition starts at higher temperatures, but in this study TGA analysis was limited up to 300°C because Therminol 66 synthetic oil is stable up to 345°C, at atmospheric conditions.

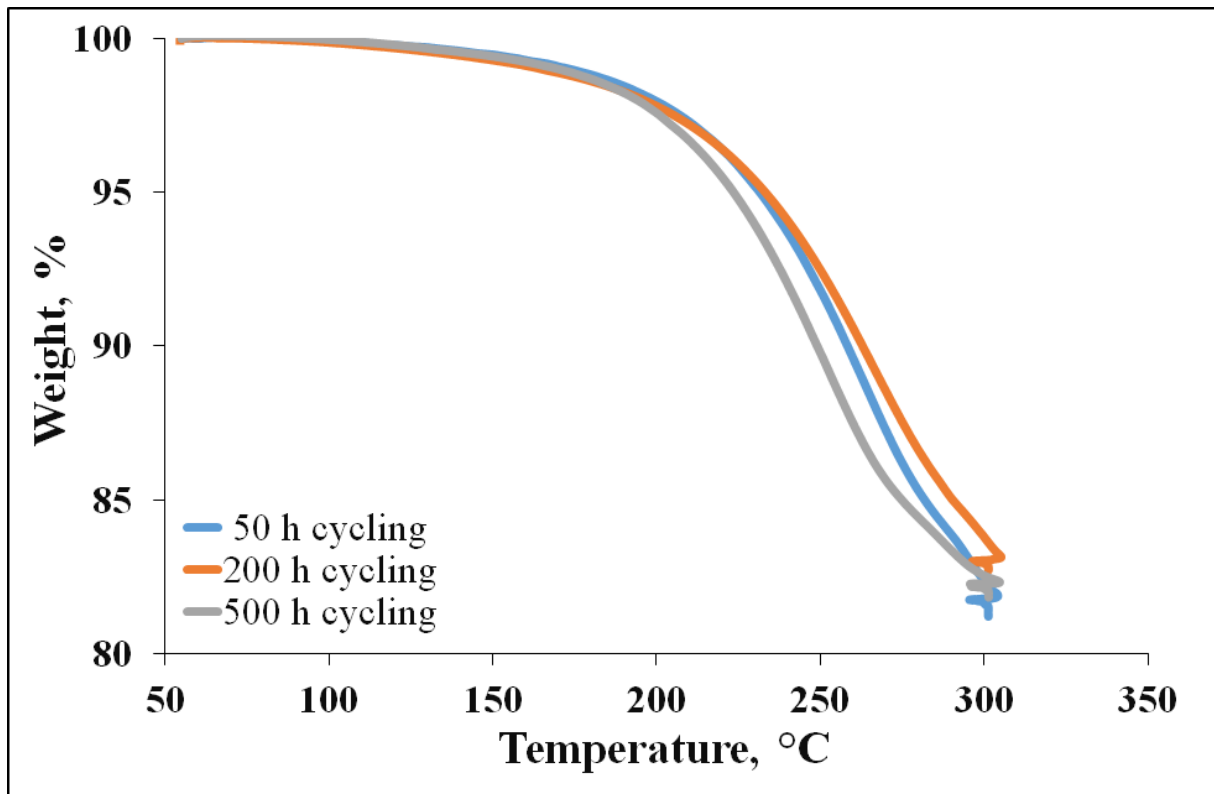


FIGURE 8 TGA measurements of spherical STESM samples after thermal cycling

STESMs in lower layers of packed-bed need to have sufficient mechanical strength to be durable under the weight of the materials above. Natural materials such as quartzite, basalt, greywacke are called hard rocks due to their high mechanical strength [2]. However, their mechanical strengths decrease after thermal cycling due to the thermal cracking occurring with increasing temperature [35]. For example, in the study by Li et al [37], micro-crack formation in granite after thermal cycling caused the strength to decrease by 69%. Micro cracks generated in the granites are due to the different thermal expansion behaviors of various mineral grains, especially in the first thermal cycle.

It is important to consider the effect of thermal cycling on the mechanical stress of new STESMs developed from DW. Compressive strength test was applied to cubic STESMs before and after thermal cycling to understand change in mechanical strength. The results show that there is an increase in the strength from 4 MPa to 6 MPa with 500 h cycling time. Figure 9 predicts the change in mechanical strength up to 1000 h by extrapolation of the regression line that shows mechanical strength can be 8 MPa after 1000h. However, the mechanical strength may remain constant after pores are saturated with oil.

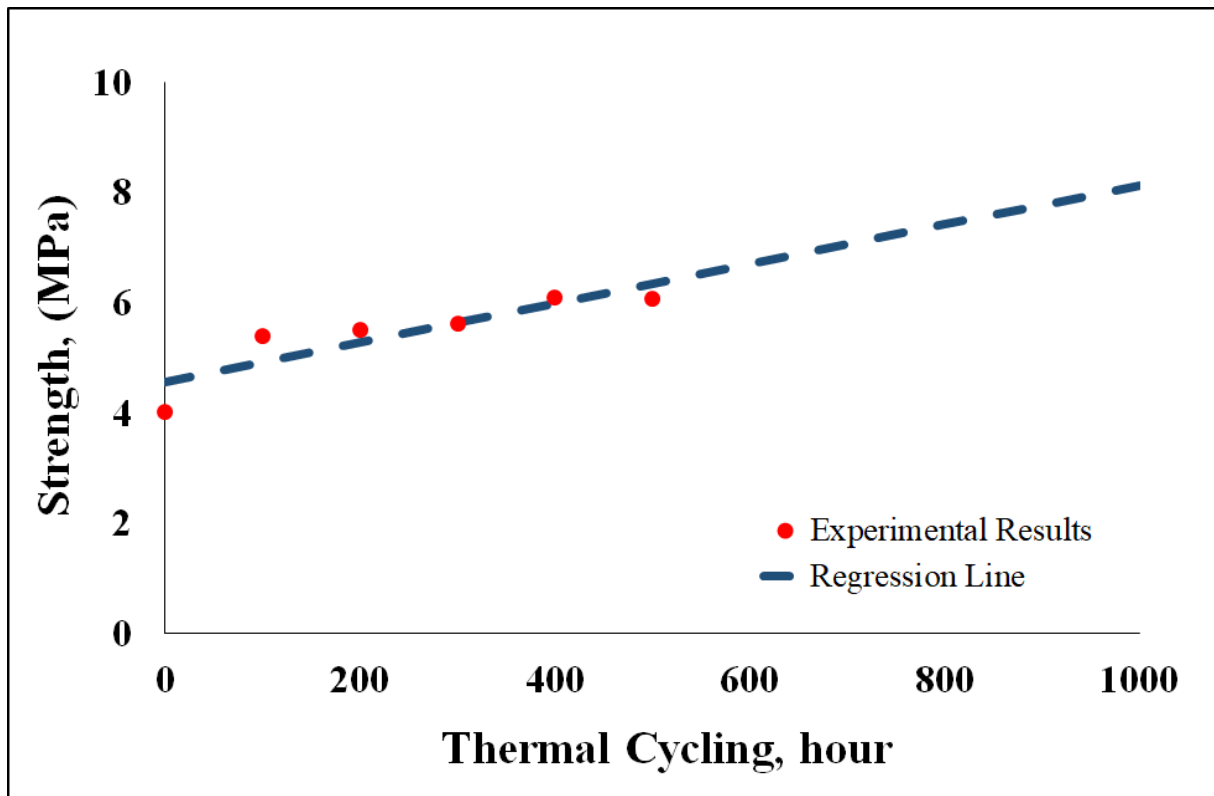


FIGURE 9 Change in mechanical strength of STESMs with cycling time

Table 6 compares the change in mechanical strength of different STESM samples before and after thermal cycling tests at different durations with STESM developed from demolition waste. As seen in Table 6, while mechanical strength of the new STESM developed from demolition waste increases with thermal cycling, for most of the natural alternative materials it decreases as a result of crack formation, enlargement of pores or chemical decomposition under hot air. In the study by Emerson et al [4], compressive strength of concrete samples decreased from 25 MPa to 5 MPa after 30 cycles at 600 °C. Riaz [49] observed no significant reduction in compressive strength after 100 h thermal cycling under hot air at 500 °C, except the granodiorite. Tiskatine et al [50] evaluated compressive strengths of different rock types for high temperature applications up to 650 °C. Results showed that Rhyolite has excellent mechanical stability during thermal cycling while compressive strength of limestone, granite and marble decreased dramatically.

STESM samples developed from demolition waste used in the lab-scale packed-bed tank of 0.9 m height and 0.3 m diameter should have mechanical strength of at least 0.02 MPa considering the storage tank volume and material's density. For large-scale systems, Allen et

al. [35] reported that storage materials with strength of 1 MPa were durable in a rock bed of 25 m height.

STESM samples after 500 h thermal cycling have acceptable mechanical strength for the lab-scale system and even for larger systems. In addition to the chemical content of the material, porosity is a parameter that affects the mechanical strength. The reduced pore volume and pore width by Therminol 66 penetration may have also increased the mechanical strength of the STESM in this study.

TABLE 6. Change in mechanical strengths of different STESM samples after thermal cycling

Material	Mechanical Strength - Initial State (MPa)	Mechanical Strength - After Cycling (MPa)	Cycling Time, h	Cycling Temp., °C	Cycling Media	Ref.
Demolition Waste	4.02	6.07	500 h	150	Therminol 66	This study
Concrete	25	5	180 h (30 cycles)	600	Air	[4]
Basalt	479	%20 reduction in compressive strength	100 h (100 cycles)	500	Air	[49]
Limestone	83	%20 reduction in compressive strength	100 h (100 cycles)	500	Air	[49]
Quartzite	512	%20 reduction in compressive strength	100 h (100 cycles)	500	Air	[49]
Granodiorite	280	%60 reduction in compressive strength	100 h (100 cycles)	500	Air	[49]
Limestone	11.4	6.9	20 h (10 cycles)	650	Air	[50]
Granite	43.1	18.5	20 h (10 cycles)	650	Air	[50]
Rhyolite	42.8	41.5	20 h (10 cycles)	650	Air	[50]
Marble	13.2	7.7	20 h (10 cycles)	650	Air	[50]

4. CONCLUSIONS

In this study, thermal behavior and service life of the new STESM were assessed using repeated heating/cooling cycles from room temperature to 150°C up to 500 h in Therminol 66 synthetic oil.

This study showed that new STESM developed from demolition wastes is thermally and mechanically stable in direct contact with Theminol 66 synthetic oil. No significant crack and porosity formation were found after thermal cycling.

The second major finding was that oil penetration improved the properties of the new STESM by lowering porosity, increasing strength and specific heat capacity. As a result of the deposition of Therminol 66 into pores of the STESM, pore width decreased slightly from 242 Å to 226 Å and density decreased from 2855 kg/m³ to 2030 kg/m³. The specific heat capacity and mechanical strength values increased from 1330 J/kgC to 1490 J/kgC and from 4 MPa to 6 MPa, respectively

It can be concluded that new STESM developed from demolition waste is a good candidate for long-term use in packed-bed STES systems for industrial solar heat applications. For further studies it is recommended to investigate the stability of new STESM with different heat transfer fluids at higher temperature ranges.

ACKNOWLEDGEMENTS

This study was carried out under a co-tutelle agreement between Cukurova University and University of Barcelona. The authors from Cukurova University thanks BAP Project (no:FDK-2018-9602), Horizon 2020 research and innovation project INPATH TES (Grant agreement ID:657466) and TÜBİTAK CSP Eranet Cofund 2019 project (Project No:120N663). The research leading to these results was partially funded by the Spanish government RTI2018-093849-B-C32 MCIU/AEI/FEDER, UE. And this study was partially funded by CSP-ERA-Net 1st Cofund Joint Call by AEI - Spanish Ministry of Science, Innovation and Universities (PCI2020-120682-2 through PCI call), TÜBİTAK - Scientific and Technological Research Council of Turkey, and CSO - Israeli Ministry of Energy. CSP-ERA-Net is supported by the European Commission within the EU Framework Programme for Research and Innovation HORIZON 2020 (Cofund ERA-NET Action, N° 838311).. A.I. Fernández would like to thank

the Catalan Government for the quality accreditation given to their research groups DIOPMA (2017 SGR 118).

REFERENCES

1. Khare S, Amico MD, Knight C, Mc Garry S. Selection of materials for high temperature sensible energy storage. *Solar Energy Materials & Solar Cells*, August 2013; 115: 114–122. <https://doi.org/10.1016/j.solmat.2013.03.009>
2. Martin C, Bonk A, Braun M, Odenthal C, Bauer T. Investigation of the long-term stability of quartzite and basalt for a potential use as filler materials for a molten-salt based thermocline storage concept. *Solar Energy*. September 2018; 171: 827–840. <https://doi.org/10.1016/j.solener.2018.06.090>
3. Molina S, Hailot D, Deydier A, Bedecarrats JP. Material screening and compatibility for thermocline storage systems using thermal oil. *Applied Thermal Engineering*. January 2019; 146: 252–259. <https://doi.org/10.1016/j.applthermaleng.2018.09.094>
4. Emerson J, Hale M, Selvam P. Concrete as a thermal energy storage medium for thermocline solar energy storage systems. *Solar Energy*. October 2013; 96: 194–204. <https://doi.org/10.1016/j.solener.2013.06.033>
5. Bruch A, Fourmigue JF, Couturiebr R. Experimental and numerical investigation of a pilot-scale thermal oil packed bed thermal storage system for CSP power plant. *Solar Energy*. July 2014; 105: 116–125. <https://doi.org/10.1016/j.solener.2014.03.019>
6. Ayappan S, Mayilsamy K, Sreenarayanan VV. Performance improvement studies in a solar greenhouse drier using sensible heat storage materials. *Heat Mass Transf.* 2016; 52: 459–467. <https://doi.org/10.1007/s00231-015-1568-5>
7. Tiskatine R, Oaddi R, Cadi R A E, et al. Suitability and characteristics of rocks for sensible heat storage in CSP plants. *Solar Energy Materials and Solar Cells*. September 2017; 169: 245–257. <https://doi.org/10.1016/j.solmat.2017.05.033>
8. Tiskatine R, Aharoune A, Bouirden L, Ihlal A. Identification of suitable storage materials for solar thermal power plant using selection methodology. *Applied Thermal Engineering*. May 2017; 117: 591–608. <https://doi.org/10.1016/j.applthermaleng.2017.01.107>
9. Diago M, Iniesta A C, Delclos T, Shamim T, Calvet N. Characterization of desert sand for its feasible use as thermal energy storage medium. *Energy Procedia*. August 2015; 75: 2113–2118. <https://doi.org/10.1016/j.egypro.2015.07.333>
10. Cascetta M, Cau G, Puddu P, Serra F. A study of a packed-bed thermal energy storage device: test rig, experimental and numerical results. *Energy Procedia*. December 2015; 81: 987–994. <https://doi.org/10.1016/j.egypro.2015.12.157>
11. Prasad L, Muthukumar P. Design and optimization of lab-scale sensible heat storage prototype for solar thermal power plant application. *Solar Energy*. November 2013; 97: 217–229. <https://doi.org/10.1016/j.solener.2013.08.022>
12. Ozrahat E, Ünalın S. Thermal performance of a concrete column as a sensible thermal energy storage medium and a heater. *Renewable Energy*. October 2017; 111: 561–579. <https://doi.org/10.1016/j.renene.2017.04.046>
13. Koçak B, Fernandez A I, Paksoy H. Review on sensible thermal energy storage for industrial solar applications and sustainability aspects. *Solar Energy*. October 2020, 209, 135–169. <https://doi.org/10.1016/j.solener.2020.08.081>
14. Alonso M C, Vera-Agullo J, Guerreiro L, Flor-Laguna V, Sanchez M, Collares-Pereira M. Calcium aluminate based cement for concrete to be used as thermal energy storage in solar

- thermal electricity plants. *Cement and Concrete Research*. April 2016; 82: 74–86. <https://doi.org/10.1016/j.cemconres.2015.12.013>
15. Navarro M E, Marti´nez M, Gil A, et al. Selection and characterization of recycled materials for sensible thermal energy storage. *Solar Energy Materials&Solar Cells*. December 2012; 107: 131–135. <https://doi.org/10.1016/j.solmat.2012.07.032>
16. Miro L, Navarro M E, Suresh P, Gil A, Fernandez A I, Cabeza L F. Experimental characterization of a solid industrial by-product as material for high temperature sensible thermal energy storage (TES). *Applied Energy*. January 2014; 113: 1261–1268. <https://doi.org/10.1016/j.apenergy.2013.08.082>
17. Faik A, Guillot S, Lambert J, et al. Thermal storage material from inertized wastes: Evolution of structural and radiative properties with temperature. *Solar Energy*. January 2012; 86(1): 139–146. <https://doi.org/10.1016/j.solener.2011.09.014>
18. Py X, Calvet N, Olives R. Recycled material for sensible heat based thermal energy storage to be used in concentrated solar thermal power plants. *Journal of Solar Energy Engineering*. August 2011, 133(3): 031008.
19. Calvet N, Gomez J C, Faik A, et al. Compatibility of a post-industrial ceramic with nitrate molten salts for use as filler material in a thermocline storage system. *Applied Energy*. September 2013; 109: 387–393. <https://doi.org/10.1016/j.apenergy.2012.12.078>
20. Agalit H, Zari N, Maaroufi M. Thermophysical and chemical characterization of induction furnace slags for high temperature thermal energy storage in solar tower plants. *Solar Energy Materials and Solar Cells*. December 2017; 172: 168–176. <https://doi.org/10.1016/j.solmat.2017.07.035>
21. Agalit H, Zari N, Maaroufi M. Suitability of industrial wastes for application as high temperature thermal energy storage (TES) materials in solar tower power plants – A comprehensive review. *Solar Energy*. September 2020; 208: 1151-1165. <https://doi.org/10.1016/j.solener.2020.08.055>
22. Fernandez I O, Calvet N, Gil A, Aseguinolaza J R, Faik A, D'Aguanno B. Thermophysical characterization of a by-product from the steel industry to be used as a sustainable and low-cost thermal energy storage material. *Energy*. September 2015; 89: 601-609. <https://doi.org/10.1016/j.energy.2015.05.153>
23. Grosu Y, Ortega-Fernandez I, Gonzalez-Fernandez L, et al. Natural and by-product materials for thermocline-based thermal energy storage system at CSP plant: Structural and thermophysical properties. *Applied Thermal Engineering*. May 2018; 136(25): 185-193. <https://doi.org/10.1016/j.applthermaleng.2018.02.087>
24. Wang Y, Wang Y, Li H, Zhou J, Cen K. Thermal properties and friction behaviors of slag as energy storage material in concentrate solar power plants. *Solar Energy Materials and Solar Cells*. August 2018; 182: 21–29. <https://doi.org/10.1016/j.solmat.2018.03.020>
25. European Commission, A European Green Deal, https://ec.europa.eu/info/strategy/priorities-2019-2024/european-green-deal_en (Access Date: 20.12.2020)
26. Koak B, Paksoy H. Using demolition wastes from urban regeneration as sensible thermal energy storage material. *Int J Energy Res*. April 2019; 43: 6454–6460. <https://doi.org/10.1002/er.4471>
27. Koak B, Fernandez A I, Paksoy H. Benchmarking study of demolition wastes with different waste materials as sensible thermal energy storage. *Solar Energy Materials and Solar Cells*. January 2021; 219, 110777. <https://doi.org/10.1016/j.solmat.2020.110777>
28. Koak B, Paksoy H. Performance of laboratory scale packed-bed thermal energy storage using new demolition waste based sensible heat materials for industrial solar applications. *Solar Energy*. November 2020; 211: 1335-1346. <https://doi.org/10.1016/j.solener.2020.10.070>

29. Attanasio, A., Largo, A., 2017. Valorization of construction and demolition wastes: RE4 building solutions, *ProScience* 4, 7-12. <https://doi.org/10.14644/amamicam.2017.002>
30. Fırat F. K., Akbaş F., 2015. İnşaat Endüstrisinde Geri Dönüşüm Çalışmalarının Geliştirilmesi ve Ekonomi Üzerine Etkileri, International Conference on Eurasian Economies Conference Proceedings, Session 4D: Çevre ve Enerji, Editors: Selahattin Sarı Alp H. Gencer İlyas Sözen, ISBN: 978-975-6319-24-6
31. Waste Framework Directive (2008/98/EC), <http://ec.europa.eu/environment/waste/framework/> [Access Date:12.03.2020]
32. Baba Y F, Ajdad H, Mers A A L, Grosu Y, Faik A. Multilevel comparison between magnetite and quartzite as thermocline energy storage materials. *Applied Thermal Engineering*. February 2019; 149: 1142-1153. <https://doi.org/10.1016/j.applthermaleng.2018.12.002>
33. Jemmal Y, Zari N, Maaroufi M. Experimental characterization of siliceous rocks to be used as filler materials for air-rock packed beds thermal energy storage systems in concentrated solar power plants. *Solar Energy Materials and Solar Cells*. November 2017; 171: 33–42. <http://dx.doi.org/10.1016/j.solmat.2017.06.026>
34. Grirate H, Zari N, Elmchaouri A, Molina S, Couturier R. Stability testing of thermal oil in direct contact with rocks used as filler material for thermal energy storage in CSP power plants. *Energy Procedia*. May 2015; 69: 860 – 867. <https://doi.org/10.1016/j.egypro.2015.03.109>
35. Allen K G, vonBackström T W, Kröger D G, Kisters A F M. Rock bed storage for solar thermal power plants: Rock characteristics, suitability, and availability. *Solar Energy Materials & Solar Cells*. July 2014; 126: 170–183. <https://doi.org/10.1016/j.solmat.2014.03.030>
36. Becattini V, Motmans T, Zappone A, Madonna C, Haselbacher A, Steinfeld A. Experimental investigation of the thermal and mechanical stability of rocks for high-temperature thermal-energy storage. *Applied Energy*. October 2017; 203: 373–389. <https://doi.org/10.1016/j.apenergy.2017.06.025>
37. Li B, Juc F, Xiao M, Ning P. Mechanical stability of granite as thermal energy storage material: An experimental investigation. *Engineering Fracture Mechanics*. April 2019; 211: 61-69. <https://doi.org/10.1016/j.engfracmech.2019.02.008>
38. Grosu Y, Ortega-Fernández I, Amo J M L, Faik A. Natural and by-product materials for thermocline-based thermal energy storage system at CSP plant: Compatibility with mineral oil and molten salt nitrate. *Applied Thermal Engineering*. May 2018; 136: 657-665. <https://doi.org/10.1016/j.applthermaleng.2018.03.034>
39. Motte F, Falcoz Q, Veron E, Py X. Compatibility tests between Solar Salt and thermal storage ceramics from inorganic industrial wastes. *Applied Energy*. October 2015; 155: 14–22. <https://doi.org/10.1016/j.apenergy.2015.05.074>
40. Naimi K M, Delclos T, Calvet N. Industrial waste produced in the UAE, valuable high-temperature materials for thermal energy storage applications. *Energy Procedia*. August 2015; 75: 2087 – 2092. <https://doi.org/10.1016/j.egypro.2015.07.320>
41. Koçak B. High temperature thermal energy storage in packed-bed – Case study in food industry. Çukurova University, PhD thesis, July 2020, Turkey)
42. Koçak B, Paksoy H. Endüstriyel Uygulamalarda Güneş Enerjisinden Termal Olarak Yararlanma. *Çukurova Üniversitesi Mühendislik ve Mimarlık Fakültesi Dergisi*, 35 (3), October 2020, 769-782 <https://doi.org/10.21605/cukurovaummf.846737>
43. Koçak B, Paksoy H. Numerical model of lab-scale packed-bed thermal energy storage system, The 13th International Renewable Energy Storage Conference (IRES 2019), *Atlantis Highlights in Engineering*, 4, November 2019, 59-63. <https://doi.org/10.2991/ires-19.2019.7>
44. Koçak B, Paksoy H. Packed-bed sensible thermal energy storage system using demolition wastes for concentrated solar power plants, *E3S Web of Conferences* 113, August 2019, 01014, SUPEHR19, 1. <https://doi.org/10.1051/e3sconf/201911301014>

45. Zahir H, Rahman M M, Irshad K, Rahman M M. Shape-Stabilized Phase Change Materials for Solar Energy Storage: MgO and Mg(OH)₂ Mixed with Polyethylene Glycol. *Nanomaterials*. 2019; 9(12): 1773. <https://doi.org/10.3390/nano9121773>
46. Chaki S, Takarli M, Agbodjan W P. Influence of thermal damage on physical properties of a granite rock: porosity, permeability and ultrasonic wave evolutions, *Constr. Build. Mater.* July 2008; 22(7): 1456–1461. <https://doi.org/10.1016/j.conbuildmat.2007.04.002>
47. Grirate H, Zari N, Elamrani I. Characterization of several moroccan rocks used as filler material for thermal energy storage in CSP power plant. *Energy Procedia*. 2014; 49: 810–819. <https://doi.org/10.1016/j.egypro.2014.03.088>
48. Xu B, Han J, Kumar A, Li P, Yang Y. Thermal storage using sand saturated by thermal-conductive fluid and comparison with the use of concrete. *Journal of Energy Storage*. October 2017; 13: 85-95. <https://doi.org/10.1016/j.est.2017.06.010>
49. Riaz M. Rock bed heat accumulators. Technical report, 1977, University of Minnesota, <https://doi.org/10.2172/6697648>
50. Tiskatine R, Eddemani A, Gourdo L, Abnay B, Ihlal A, Aharoune A, Bouirden L. Experimental evaluation of thermo-mechanical performances of candidate rocks for use in high temperature thermal storage, *Applied Energy*, 171, June 2016, 243-255, <https://doi.org/10.1016/j.apenergy.2016.03.061>.